HAN_UNIVERSITY
OF APPLIED SCIENCES

Minor Project - Applied Control
The Process of Popping Rice Waffles

Master Engineering Systems

PREFACE

Slagman Techniek specializes in machine building and caters to various industries. One of their machines creates rice waffles by heating a small amount of rice in a closed cylinder until it 'pops'. They are seeking to improve the machine's performance and as a part of that process they want to create their own controller for the heating and pneumatic system.

A team of systems engineering students has accepted the challenge to do so and subsequently delivered a prototype controller with the help of lecturers and bachelor students from the HAN University of Applied sciences and Kees van Cappellen from Slagman. The team would like to thank Ad Oomen, Richard Kaandorp, Kees van Cappellen, Jasper Lankhorst and Jelle van Putten for their assistance throughout the project.

Project title: "The Process of Popping Rice Waffles"

Name of students:	Thad Popan (1678795) Daan Lubbers (1573167) Osatohanmwen Owieadolor (2107064) Pim Jansen (1598251)
Company:	Ad Oomen and Kees van Cappellen on behalf of Slagman Techniek
HAN Supervisor:	Richard Kaandorp (Ad Oomen)
Date:	2023, June 14

SUMMARY

Slagman Techniek B.V. is the manufacturer of a rice popping machine used by one of their clients, Sanorice, to produce rice waffles. The machine does so by superheating a rice mixture within a cylindrical cooking chamber at 280°C for 10 seconds. This in turn allows the water within the rice to expand forming a waffle, which pops out of the machine. Sanorice has noticed that the machines consume a lot of energy during operation and as a result, has brought this concern to Slagman Techniek. Therefore, Slagman Techniek would like to investigate the problem and potentially improve on the machine's power consumption or cycle time.

As a part of this effort Slagman has reached out to the HAN to develop a controller for the heating and pneumatic system of the machine, so that they could independently investigate, experiment and iteratively improve their machine internally. The goal for this project is to take over the temperature and pneumatic controls of the machine with an Olimexino microcontroller. The controller should be robust and be portable to different machine variants.

To start with a literature review is performed to learn more about the operation of the machine and about different types of control systems and tuning methods which could be used. Afterwards a thermal model of the system is developed in Matlab Simulink. A white box model for a simplified representation of the system consisting of a set of energy balances was developed, as well a black box model fitted to measurements taken from a test machine. Several assumptions were made for the white box modelling and it was validated against measurements from the test machine.

After the modelling phase a controller is designed and simulated in Matlab Simulink. Several options were considered such as a PD, PI, PID, feedforward, and fuzzy controller. Given the complexity of the project and the limited time a PID controller was deemed the most feasible to create a prototype with and should meet the requirements. However, the D component was dropped because it could cause issues with sensor noise during the implementation. First the root locus method is used to analyze the stability of the system, then the built-in tuner within Simulink was used to optimize the P & I values of the controller.

Finally a controller implementation is realized using an Olimexino microcontroller to control both the temperature feedback loops of the top and bottom cooking plates, and the six pneumatic cylinders. The controller values derived from the simulations were used as a starting guide and tuned further using a slope-based method. There was insufficient time to perform exhaustive experiments with the prototype, but several test runs were done and the machine was able to produce rice waffles at the expected quality. The temperature fluctuated between 279ºC and 289ºC which is significantly less than with the original controller.

At the end this resulted in a set of recommendations which Slagman can use to move forward with their program of overhauling the rice poffer. The hardware and software setup should be improved, and the controller needs to be tuned better. The controller should also be validated in different circumstances and environments. More advances control techniques such as feed-forward or two-phase controllers could also be considered.

Table of Contents

1. INTRODUCTION

1.1 Background

Slagman Techniek has designed a machine for their client Sanorice, which is used to make rice waffles (Figure 1). This machine heats a combination of rice grains, water, sesame seeds and salt between two heated circular plates to convert this combination of materials to a waffle. During the heating phase, the water within the mixture is superheated, which in turn causes a change in structure, releases the starch, and increases the volume of the product and pressure between the plates. This resulting pressure causes the rice to pop, and subsequently produces a rice waffle. The entire process takes approximately 10 seconds depending on the size of the waffle being made.

Sanorice has two different types of rice waffles, a large one with 10 cm diameter and a smaller variant with a diameter of 4 cm. The larger waffle has a thickness of 1 cm while the smaller waffle has a thickness of 0.5 cm. The machine used to create both variants are similar and operate in a similar manner. The only major differences are the weight of rice used and the size of the molds used to heat the rice. Sanorice has determined that the operation of these machines consumes a lot of power.

Due to the high power consumption, Slagman Techniek is looking to optimize the popping process by improving the controllability of the process and redesigning key components. Two bachelor students from the HAN University of Applied Sciences are responsible for the redesign and are researching the pneumatic and thermal properties of the machine. The scope of this project is to create a model of the popping process and to design a robust temperature controller to control and improve the temperature during the popping process. The team will also look into the possibility of creating a controller for the pneumatics of the system. The team will focus on the machine which creates the larger waffles.

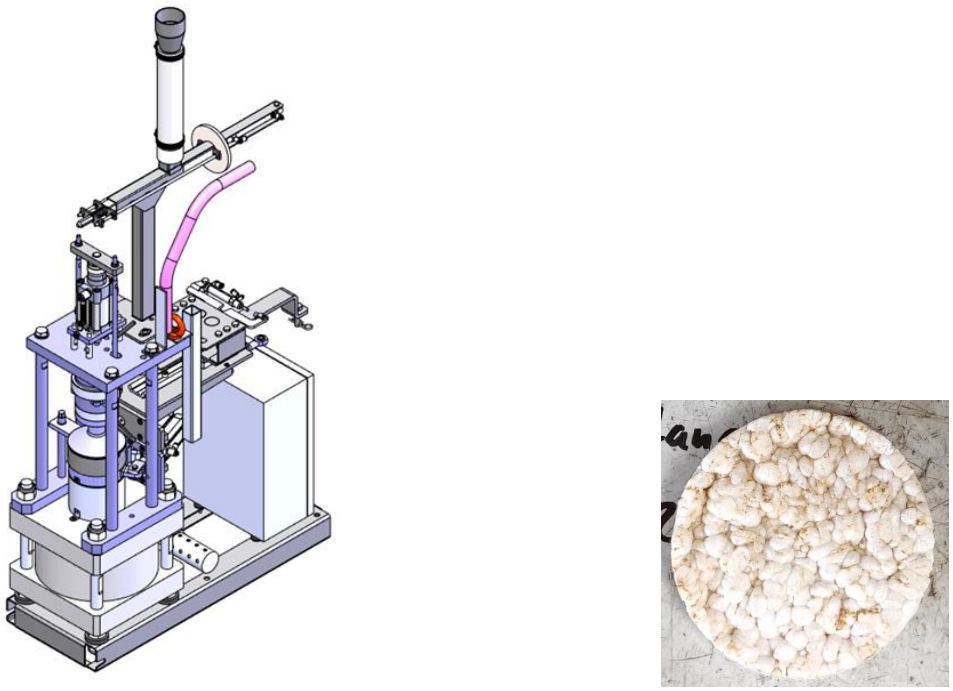

Figure 1 Left: Slagman rice popping machine; Right: Waffle example (Source: Slagman Techniek B.V.)

1.2 Problem definition

The popping process of the rice waffles does not meet the required yield and energy consumption requirements by Sanorice. Initial investigation has indicated that the temperature control of the machine uses an on-off controller based on a lower threshold. Furthermore, the pneumatics of the machine is operated as an open loop system. The client would like to be less dependent on the current supplier of the software for the process control. The controller for the machine must be sufficiently robust as to negate the effects of external disturbances such as:

1. Contamination of the machine during its operation
2. The humidity level within the rice
3. Ambient temperature variations
4. Discontinuities within the process

The controller should also be backwards and forward compatible across the different machine variants.

1.3 Project objectives

The main goal of the project is to create a temperature and pneumatic controller for the Slagman test machine setup in their workshop. To attain this goal the following objectives are formulated:

- Understand the popping process and determine the important parameters.
- Develop a thermal model of the popping process in Matlab Simulink.
- Develop a temperature controller for the popping process in Matlab Simulink.
- Develop an open loop control for the pneumatics for the popping process.
- Implement the control system on an Olimexino microcontroller and validate it using the test machine in the Slagman workshop with an Olimexino

1.4 Research question

To solve the problems outlined by Sanorice and Slagman the below research questions are formulated.

Main Question:

How can the temperature control of the Slagman machine be optimized to improve the production yield of the rice waffles and reduce the energy consumption?

Sub-questions:

1. What are the parameters and the conditions for the popping process?
2. How can the temperature be controlled while the machine is in operation?
3. How robust is the controller?
4. How can the improved temperature control affect the process cycle?

1.5 Approach

The best way to achieve the desired result of a temperature and pneumatic controller implementation is to take an iterative approach towards solving the problem. The initial modelling, controller design, and controller implementation will start simple so that a rapid prototype can be realized in a short timeframe. Throughout the project timeframe the knowledge and understanding of the process will increase and more complex methods could be tried if time permits.

1.6 Outline of the minor project report

Chapter 2 discusses the results of the literature review. Chapter 3 describes the method used to obtain the results from chapter 4. The conclusion is given in chapter 5. Finally the recommendations resulting from the project are summed up in chapter 6. At the end the references and appendices can be found.

2. LITERATURE SURVEY

To start with a literature survey is performed to gain understanding of the concepts required to develop a controller for the machine. This outcome of this research phase is summarized in this chapter.

2.1 Operation of the machine

The rice popping machine consists of several subsystems which are then assembled together and tested by Slagman. Due to the scope of this project the team will only focus the research on the following two systems which are highlighted in Figure 2:

1. Pneumatic system
2. Heating system

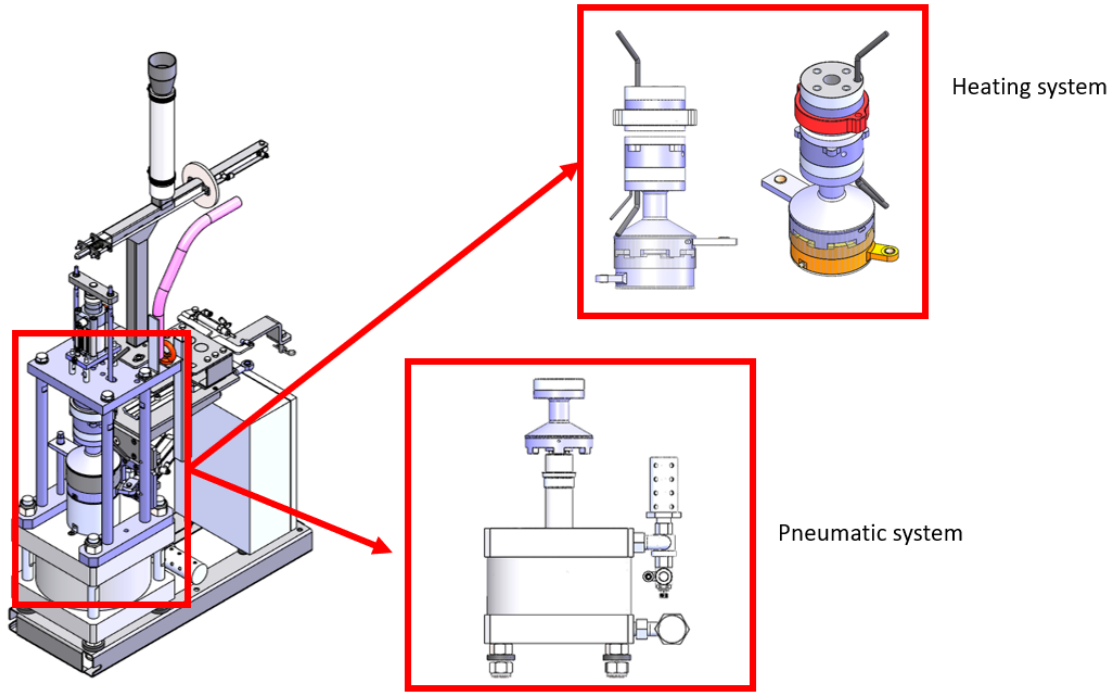

Figure 2 Hardware of the heating and pneumatics systems (Source: Slagman Techniek B.V.)

The rice popping machine operates using heat and pressure to turn a rice grain mixture into a rice waffle. To do so the machine uses a pneumatic system to open and close the cooking chamber, a feeder system to place the correct quantity of rice into the cooking chamber and also a heating system to cook the rice. The particular mechanism can vary depending on the specific design and technology used.

During operation the cooking chamber is sealed using the pneumatic system, creating a controlled environment for the rice to "pop". The cooking chamber is then heated to 280°C . The high temperature causes the moisture inside the rice grains to turn into steam, which builds up pressure inside the chamber. The pressure and heat cause the rice grains to expand and burst open, creating the characteristic popcorn-like texture. The chamber is made of a stainless steel alloy, which is designed to withstand high cooking temperatures and pressures. Once the rice grains have popped, the machine will automatically move the resulting waffle from the heating plate.

The heat transfer behavior of the rice popping machine and its components is characterized by the flow of heat from the heating element to the rice grains. The temperature of the heating element must be carefully controlled to ensure that it does not overheat or burn the rice grains. The chamber

and lid also play a critical role in heat transfer by trapping the heat and pressure inside, allowing the rice grains to cook evenly and pop without bursting.

2.2 Limitations in control of the machine

To isolate the areas of improvement the two control systems of interest of the Slagman machine, namely the pneumatic and the heating system, are examined. A summary is given in Table 1.

	System	Use	Type of control	Remarks
1	Pneumatic system	Used to open and close the cooking chamber of the machine and to feed the rice.	Open loop	The operation of this system is time based. Thus, there is no communication with the heating system. This means that if there is any variation in the temperature it could easily result in either undercooked or overcooked rice waffles. Depending on whether the temperature is too high or too low.
2	Heating system	Used to heat the rice and maintain a cooking temperature of 280°C	Closed loop	The heating elements supplies power to maintain a set temperature of 280°C. However with the current controller the temperature can vary a large amount.

Table 1 Control systems of the machine

2.3 Types of control systems

There are three (4) types of control systems considered for the application on the Slagman Machine:

- Open loop
- Closed loop (Feedback)
- Feed-forward
- Fuzzy control

Each control system has their advantages and disadvantages based on the area of application which are described below.

Open loop: In this type of control system, the output is not measured and fed back into the system. Furthermore, in this system the condition of the output is not measured or monitored. As a result the output of the system has no influence on the input which means it is unable to "self-correct" or adjust to varying disturbance or external changes. This is the major drawback of using an open loop system. As a result extra supervisory attention is needed to ensure that the output remains within its specified limits. Due to the limitations of an open loop system, it would not be able to provide the required improvement in the machine performance.

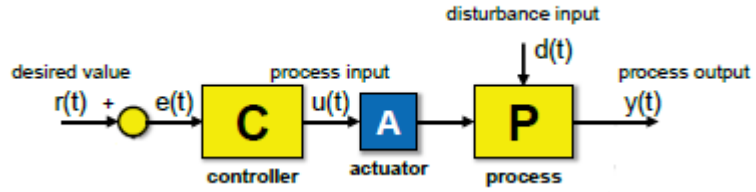

Figure 3 Open loop control system [1]

Closed Loop (Feedback): This type of controller measures the output of the process, and subsequently manipulates the input to drive the process to a desired set point. For this system to work effectively there should be sensors to accurately measure the output of the system. If this is possible then closed loop control can more closely match the process output to the desired value, depending on the system.

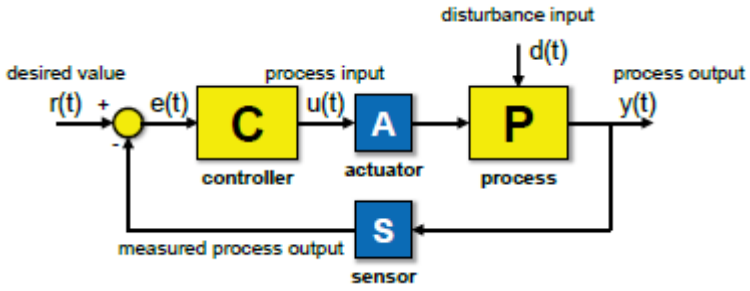

Figure 4 Closed loop control system (Feedback) [1]

Feed Forward: This type of controller can anticipate the effect of a disturbance that could in turn affect the process. This type of controller would sense and compensate for the disturbance before it affects the process. This type of controller is more accurate than a Feedback controller but only works for disturbance rejection if the disturbance is exactly known. This type of controller could be considered in the future because the rice draws heat cyclically at known points.

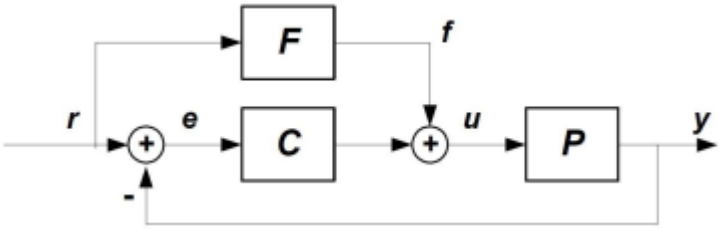

Figure 5 Feed forward system [2]

Fuzzy Controller: A fuzzy controller could be used in the design of a controller for a rice popping process machine to regulate and optimize the popping process, the concept is illustrated with an example below.

Input Variables:
Temperature: Measured temperature inside the popping chamber.
Pressure: Measured pressure inside the popping chamber.
Moisture: Measured moisture content of the rice grains.

Output Variable:
Heating Power: Control signal to adjust the heating element of the machine.

Fuzzy Sets:
For each input variable, define fuzzy sets that represent different levels or ranges of the variable. For example, "Low," "Medium," and "High" for temperature, pressure, and moisture.

Fuzzy Rules:
Establish a set of fuzzy rules that define the relationship between the input variables and the output variable. These rules are typically defined based on expert knowledge or empirical data. For example: IF Temperature is High AND Pressure is Low AND Moisture is High THEN Heating Power is Low.

Fuzzy Inference:
Apply fuzzy inference to determine the appropriate output based on the fuzzy rules. This involves evaluating the degree to which each rule is satisfied based on the current input values.
Defuzzification:
Convert the fuzzy output into a crisp value that can be used as the control signal for the heating power. This can be done using various methods, such as centroid or maximum membership.

By utilizing a fuzzy controller, the rice popping process machine can adjust the heating power based on the measured temperature, pressure, and moisture levels. The fuzzy rules and fuzzy inference engine enable the controller to make intelligent decisions and adapt to different operating conditions, optimizing the popping process and achieving desired results such as consistent popping, controlled browning, and efficient energy usage.

S/N	Case	Used alongside	Functions	References
1.	To control the movement speed for a rice transplanter for navigation and precision	A PID controller	Adaptive control with changes of set point and engine speed	[3]
2.	Design and experiment on intelligent fuzzy monitoring system for corn planters	A DC Motor	Precisely correlates a stepless spacing regulator used in a non-linear system and can be described by a pure-time delay.	[4]

Table 2 Sources for fuzzy controller applications

2.4 Controller tuning methods

Both when simulating the controller and when implementing the controller on the test machine it is likely that the controller parameters need to be tuned to achieve the desired system response. To do so the controller must be tuned and there are a few methods which could be used. Some methods which are interesting for use during this project are discussed below.

Ziegler-Nichols method:
This is a simple tuning method where the focus is on determining the ultimate proportional value K_u. While doing so the gain values for the I and D factors should be zero. To do so the operator should increase value of the proportional constant until reaching K_p, until sustained oscillations around the setpoint are seen. Then the ultimate period of oscillation P_u should be determined. The operator can then use K_u and P_u along with the Ziegler-Nichols closed loop equations ((1) and Table 3) to determine the controller settings [5].

$$(1)\ U(t) = K_c \left(\epsilon(t) + \frac{1}{\tau_i} \int_0^t \epsilon(t')dt' + \tau_d \frac{d\epsilon(t)}{dt} \right)$$

	K_c	τ_i	τ_d
P	$K_u/2$		
PI	$K_u/2.2$	$P_u/1.2$	
PID	$K_u/1.7$	$P_u/2$	$P_u/8$

Table 3 PID constants using Ziegler-Nichols method [5]

Chien-Hrones-Reswick:
This tuning method is based on Ziegler-Nichols and is based on an open-loop step response measurement. It works well for higher order systems with a significant delay. The delay and rise time are measured, as well as the ratio of the changes in input/output from which the controller values can be calculated. Values can be calculated for no overshoot or 20% overshoot [6] [7].

Simulink Built-in tuner:
Matlab Simulink has a built in tuner in the PID controller block which could be used to determine the controller settings to achieve the desired response. Using this tuning method is fairly simple. However, the calculated value by the Simulink tuner could also might not deliver exactly behavior desired by the designer, thus the values derived from the tuner should be used as a starting point, where the designer could vary the values until the desired behavior is achieved.

Figure 6 PID controller block from Simulink

3. METHODS

The methods which will be used to obtain the results are described and motivated in this chapter. First the a general overview and justification of the research design are presented. Afterwards the detailed methods for the white box modelling process are described.

3.1 Description of research design

The project is broken down into five phases which are listed in Table 4. For each phase the description and results are given.

Phase number	Title	Description	Deliverables
1	Initialization	Dissecting the problem faced by the client. The team needs to ensure that the problem is clear and that the proposed solution and way forward contribute to solving the problem.	• Project plan • Clarified scope
2	Literature review	Reviewing articles and conducting interviews with experts to determine the operation of the machine and the various types of control systems. The team will also use this phase to understand the application of the Olimexino microcontroller for the implementation.	• Understanding the machine processes and operation • Understanding the operation of the various types of control systems • Understanding the application of the Olimexino
3	Modelling	The thermal process will be modelled using both white-box and black-box modelling methods following the 4+1 approach [1]. The equations will be used to construct a Simulink model and create a MATLAB file. The model will be split into various sub-systems for readability.	• Process definition • Data flow diagram • Equations • Simulink model of the system
4	Simulation & Controller Design	Simulations will be done to validate the model by comparing it to measurements taken from the machine. Then the controller will be designed using simulations to validate the controlled system response.	• Validated model • Thermal Controller
5	Realization	Finally the controller will be realized on the test poffer machine in the Slagman workshop. The controller software will run on an Olimexino and interfaces with the existing hardware.	• Prototype thermal and pneumatic controller setup

Table 4 Description of research design

3.2 Justification of research design

Several research questions are posed in order to investigate the problem at hand. Answering these questions will help reach the goal of designing a controller and using the Olimexino microcontroller to control the machine. Table 5 shows the justification for the research questions.

Number	Research question	Method of solving	Justification	Remarks
1	What are the parameters and the conditions for the popping process?	Literature study and interviews to learn about the operation of the Slagman machine and the processes used at Sanorice to make rice waffles.	Research into the mechanics and operation of the machine will allow the team to better understand the machine and the process of making rice waffles.	
2	How can the temperature be controlled while the machine is in operation?	Literature study and simulating the process. Finally it should also be experimentally tried on the machine.	To determine the best possible method to control the temperature of the machine and reduce its power consumption.	
3	How robust is the controller?	This question will be solved by simulating the controller in scenarios with varying disturbances.	The controller should be sufficiently robust so that external disturbances has a negligible effect on the process.	The most important disturbance affecting the process is the heat consumed by the rice while it heats up.
4	How can the improved temperature control affect the process?	Running simulations and tests on the machine with the designed controller.	To determine whether the improved control has any effects on yield or quality of the product.	The goal of the project is to reduce power consumption and positively improve the yield. Thus, the team needs to monitor the effect of the changes implemented.

Table 5 Justification of research design

3.3 White box modelling of the thermal process

To obtain a model which can be used for controller design and simulation a white box model is developed using the 4+1 approach [1]. This section describes how the model is created and validated. The model is based on a simplified representation of the device that can be seen in Figure 7. Two states are considered, one in which the ring is up and no rice is being cooked, and one in which the ring is down and rice is being cooked.

Each element is modelled as a solid cylinder (or ring) consisting of one material. In the actual device this is not the case as there are small features and there are also bolts, the coil, and the sensor embedded within the cylinder. However, the main thermal mass for each element is made up of a single material and by making this assumption the modelling using differential equations is greatly simplified.

For the model any elements that come after the isolation are disregarded, and instead the isolation is assumed to lose heat to surrounding air via convection as if there was nothing connected behind it. The isolation provides a break in thermal conductivity. Test results show that the steady state temperature of elements beyond the isolation are a lot lower than elements before it (~250C against 50-100C) [8].

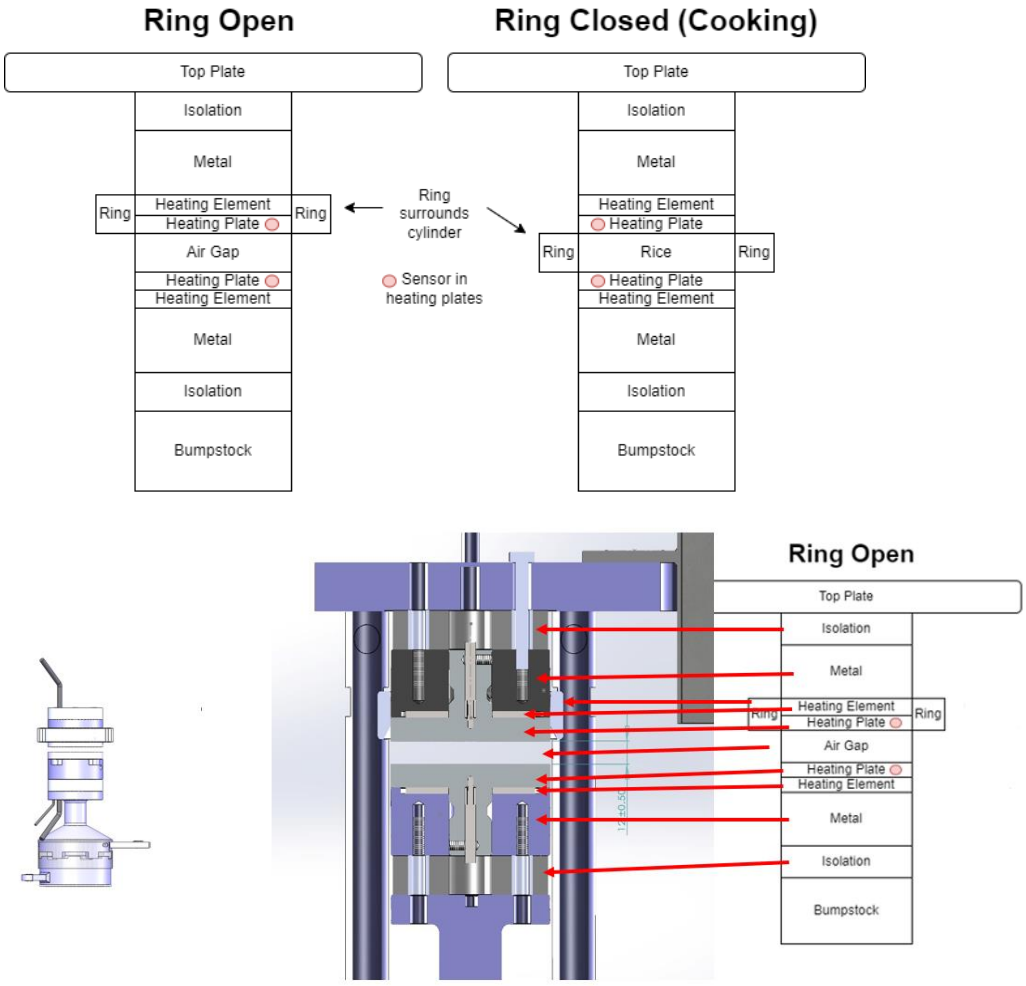

Figure 7 Top: Device Schematic; Bottom: Device Schematic mapped onto the 3D model

3.3.1 Defining the process

The process definition is given in Table 6. The balances in the system are all the energy balances between the different elements shown in the schematic. The storages in the system are the temperatures between the different elements.

Goals for Control	• The temperature [C] of the top heating plate equals the setpoint Temperature [C]. • The temperature [C] of the bottom heating plate equals the setpoint Temperature [C].
Process Outputs	• The top heating plate temperature [C] measured by the thermocouple sensor. • The bottom heating plate temperature [C] measured by the thermocouple sensor.
Control Inputs	• The top heating coil power [W] controlled by a PWM signal. • The bottom heating coil power [W] controlled by a PWM signal.
Major Disturbances	• The ambient temperature [C]. • The power [W] consumed for the heating of the rice. • The movement of the ring. Note: the effect of the contamination on the machine is assumed to be negligible based on temperature measurements from both the clean and dirty machines. Hence it was not considered as a disturbance here. [8]

Table 6 Process Definition

3.3.2 Data flow diagram

Figure 8 shows the data flow diagram. The heat flows through the different elements starting at the coil, which heats up based on the applied power, and from there it is transferred to the heating plate, the metal section, and the isolation. For the top part of the cylinder the heat can also be transferred to the ring depending on the ring position. In the end the sensors measure the heating plate temperature.

Each element except for the heating coil gives off heat to the ambient air. In the actual construction the heating coil is not exposed to the air, so this only gives off heat to the metal and heating plate layers.

It is assumed that the heating of the rice only withdraws heat from the two heating plates as the rice is dropped in the center of the heating plates and the surface area of the inside of the ring is comparatively small.

The temperatures are defined in the positions as denoted in Figure 9. The heating coil is assumed to have a uniform temperature since it is small and actively heated. The other temperatures are defined on the surfaces away from the coil, the temperature on each surface is assumed to be uniform. It is assumed that within each element is a linear temperature gradient between both sides.

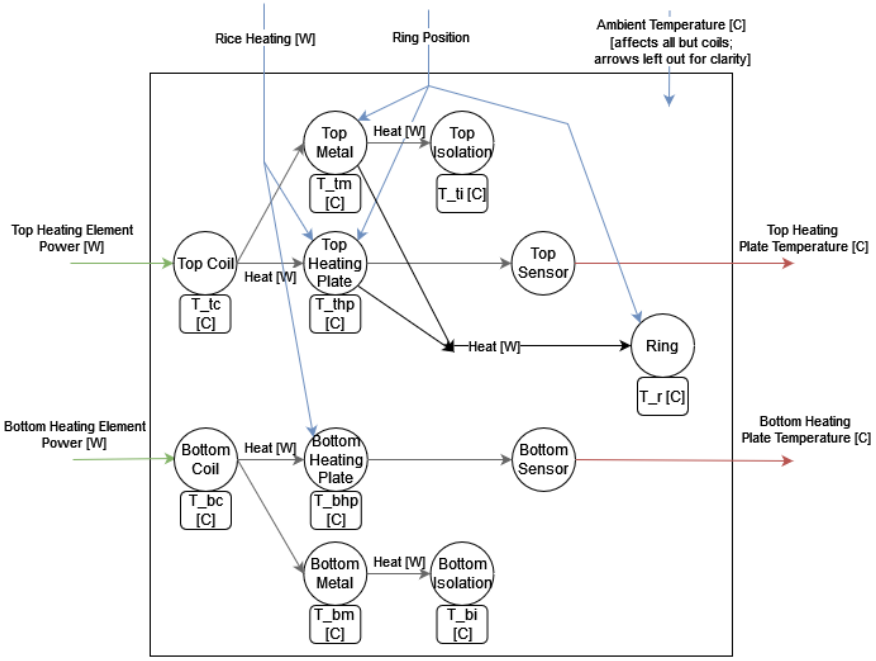

Figure 8 Data Flow Diagram

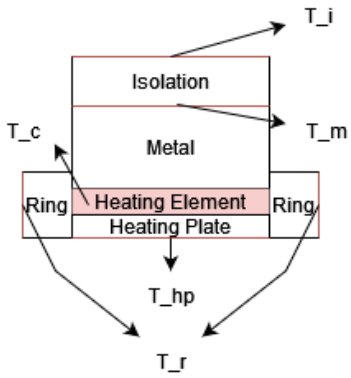

Figure 9 Temperature Definition

3.3.3 Modelling equations

Each of the below equations is an energy balance which includes conduction between elements, convection between elements and the ambient air, as well as power input and power loss through heating the rice. The effect of radiation is assumed to be negligible, because for an ideal radiator with a temperature of 285ºC and an area of 0.0375m² (which is comparable to the area of the modelled elements exposed to the air) the radiated power is only 14W.

The parameter list for all the equations can be found in Appendix A.

(2) is the energy balance for the top coil, and (3) for the bottom coil. Heat is added based on the applied voltage and current $P_c = I^2R$. The heat loss Heat is lost through conduction with the adjoining metal and heating plate layers.

$$(2)\ m_{tc}c_{tc}\dot{T}_{tc} = P_{tc} - \frac{k_{tm}}{d_{tm}}A_{tm}(T_{tc} - T_{tm}) - \frac{k_{thp}}{d_{thp}}A_{thp}(T_{tc} - T_{thp})$$

$$(3)\ m_{bc}c_{bc}\dot{T}_{bc} = P_{bc} - \frac{k_{bm}}{d_{bm}}A_{bm}(T_{bc} - T_{bm}) - \frac{k_{bhp}}{d_{bhp}}A_{bhp}(T_{bc} - T_{bhp})$$

(4) is the energy balance for the top metal with the ring down, (5) with the ring up, and (6) for the bottom metal. For all three heat is added through conduction from the coil and heat is lost through conduction to the insulation and convection to the ambient air. When the ring is up, the area exposed to the air is reduced and instead of that heat is lost through conduction to the ring.

$$(4)\ m_{tm}c_{tm}\dot{T}_{tm} = \frac{k_{tm}}{d_{tm}}A_{tm}(T_{tc} - T_{tm}) - \frac{k_{ti}}{d_{ti}}A_{ti}(T_{tm} - T_{ti}) - h_c A_{tm_{air}}(\frac{T_{tc}+T_{tm}}{2} - T_a)$$

$$(5)\ m_{tm}c_{tm}\dot{T} = \frac{k_{tm}}{d_{tm}}A_{tm}(T_{tc} - T_{tm}) - \frac{k_{ti}}{d_{ti}}A_{ti}(T_{tm} - T_{ti}) - h_c(A_{tm_{air}} - A_{r_{tm}})\left(\frac{T_{tc}+T_{tm}}{2} - T_a\right) - \frac{k_r}{d_r}A_{r_{tm}}(T_{tm} - T_r)$$

$$(6)\ m_{bm}c_{bm}\dot{T}_{bm} = \frac{k_{bm}}{d_{bm}}A_{bm}(T_{bc} - T_{bm}) - \frac{k_{bi}}{d_{bi}}A_{bi}(T_{bm} - T_{bi}) - h_c A_{bm_{air}}(\frac{T_{bc}+T_{bm}}{2} - T_a)$$

(7) is the energy balance for the top isolation, and (8) for the bottom isolation. Heat is added through conduction from the metal and heat is lost through convection to the ambient air, on both the sides and the top/bottom.

$$(7)\ m_{ti}c_{ti}\dot{T}_{ti} = \frac{k_{ti}}{d_{ti}}A_{ti}(T_{tm} - T_{ti}) - h_c A_{ti_{air}}\left(\frac{T_{tm}+T_{ti}}{2} - T_a\right) - h_c A_{ti}(T_{ti} - T_a)$$

$$(8)\ m_{bi}c_{bi}\dot{T}_{bi} = \frac{k_{bi}}{d_{bi}}A_{bi}(T_{bm} - T_{bi}) - h_c A_{bi_{air}}(\frac{T_{bm}+T_{bi}}{2} - T_a) - h_c A_{bi}(T_{bi} - T_a)$$

(9) is the energy balance for the top heating plate with the ring down, (10) with the ring up. (11) and (12) are those for the bottom heating plate. For all these energy balances heat is added through conduction from the coil, and heat is lost through convection with the ambient air. With the ring down, heat is also consumed by the rice being heated. With the ring up instead, heat is lost on the rice facing surface to convection with the ambient air. When the ring is up, the top heating plate loses heat from conduction to the ring on its side surface.

$$(9)\ m_{thp}c_{thp}\dot{T}_{thp} = \frac{k_{thp}}{d_{thp}}A_{thp}\left(T_{tc} - T_{thp}\right) - h_c A_{thp_{air}}\left(\frac{T_{tc}+T_{thp}}{2} - T_a\right) - P_{rice}$$

$$(10)\ m_{thp}c_{thp}\dot{T}_{thp} = \frac{k_{thp}}{d_{thp}}A_{thp}\left(T_{tc} - T_{thp}\right) - \frac{k_r}{d_r}A_{thp_{air}}\left(T_{thp} - T_r\right) - h_c A_{thp}\left(T_{thp} - T_a\right)$$

$$(11)\ m_{bhp}c_{bhp}\dot{T}_{bhp} = \frac{k_{bhp}}{d_{bhp}}A_{bhp}\left(T_{bc} - T_{bhp}\right) - h_c A_{bhp_{air}}\left(\frac{T_{bc}+T_{bhp}}{2} - T_a\right) - P_{rice}$$

$$(12)\ m_{bhp}c_{bhp}\dot{T}_{bhp} = \frac{k_{bhp}}{d_{bhp}}A_{bhp}\left(T_{bc} - T_{bhp}\right) - h_c A_{bhp}\left(T_{bhp} - T_a\right) - h_c A_{bhp_{air}}\left(\frac{T_{bc}+T_{bhp}}{2} - T_a\right)$$

Finally, (13) is the energy balanced for the ring in the up position, and (14) in the down position. In the up position the ring is heated through conduction by the metal and the heating plate, and in both positions heat is lost through convection with the ambient air.

$$(13)\ m_r c_r \dot{T}_r = \frac{k_r}{d_r}A_{r_{tm}}(T_{tm} - T_r) + \frac{k_r}{d_r}A_{thp_{air}}\left(T_{thp} - T_r\right) - h_c A_{r_{air}}(T_r - T_a)$$

$$(14)\ m_r c_r \dot{T}_r = -h_c A_{r_{air}}(T_r - T_a)$$

3.3.4 Selecting the linearization method

For the feedback controller design a transfer function is used. However, the model has initial conditions and will be non-linear because of constant terms resulting from the ambient temperature. Transfer functions only apply to linear systems without initial conditions. To find the transfer function for the model the validated model will be simulated without initial conditions, and then the Matlab function 'tfest' for estimating transfer functions from input-output data will be used. Any linearization should be done around the operating point of 280°C.

3.4 Black box modelling

In order to obtain a black box model, the dataset in Appendix B is used and first has to be made usable. This dataset uses the wattage as input and the temperature as output and is loaded into Matlab as a matrix. Afterwards this the data is cleaned and interpolated. Then the System Identification tool in Matlab is used to read in this dataset. Here, the estimated number of poles and zeroes can be entered. Iteratively the best fit percentage is found. The results are described in paragraph 4.2.

3.5 Selecting the model validation method

The models are validated with the measurements which were available from the machine that is sitting in the Slagman workshop. The validation data includes input power and measured heating plate temperature for both a heat up cycle and a longer-term steady state measurement. The data is given in Appendix B. There are not a lot of datapoints for the input power so it is linearly interpolated between the datapoints.

3.6 Modelling the rice disturbance

While the rice is cooking it absorbs heat from the heating plates and the ring. It is a cyclic pattern which is modelled as a 3 second cooking period during a 12 second production cycle. During steady state production the total machine consumes 700W extra compared to a steady state without production [8]. By making the assumption that the heat absorbed by the rice accounts for this extra energy usage it can be seen that 2800W is extracted during the 3 seconds of cooking, which equates to 1400W per heating plate.

4. RESULTS

In this chapter the results of the modelling, controller design, simulations and implementation are described. All Matlab files used for producing the results can be found in Appendix D.

4.1 White box model

Figure 10 shows the white box Simulink model. Each energy balance equations is implemented in one of the subsystem blocks. For example the top heating plate model is shown in Figure 11. The power consumed by heating the rice is divided proportionally between the two heating plates. Within the subsystems, switch blocks are used to switch between the differential equations for the ring up situation (when P_rice is 0) and the ring down situation.

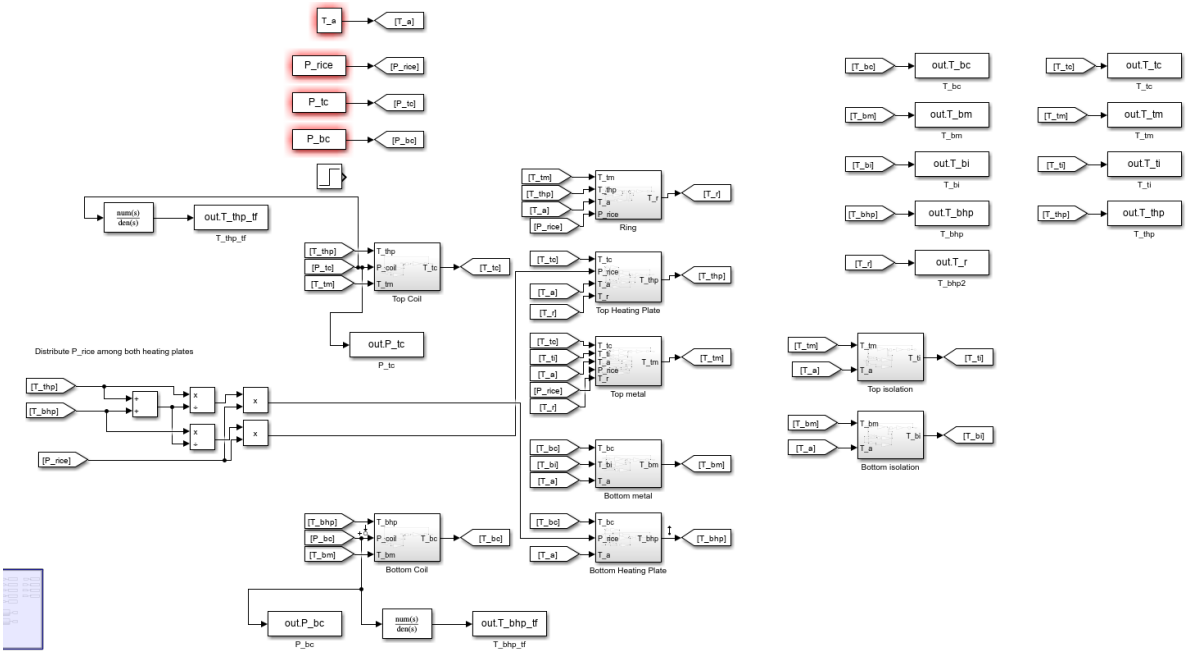

Figure 10 White Box Simulink Model

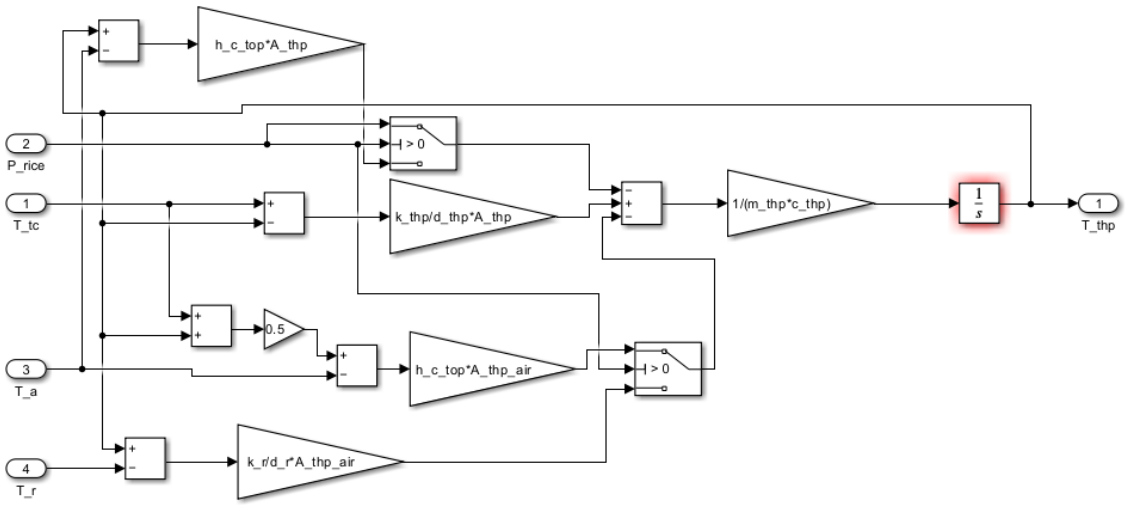

Figure 11 Top heating plate Simulink model

4.1.1. Validating the white box model

Figure 12 shows the validation results of the model. The simulated temperatures are overlaid with the measured temperatures. On the right-axis the coil power input is shown. The model is a good match for both the steady-state value as well as the heat up cycle, considering the accuracy of the measurements and the fact that a robust controller is being developed. The validation data is given in Appendix B.

The air convection coefficient has a big impact on the simulated temperature, but this is a value which is not known. So the coefficients were tuned separately for the top and bottom section in order to provide the best match between the model and the measurement. This was done by varying the coefficient to minimize the sum of squared errors between the simulation and the measurements.

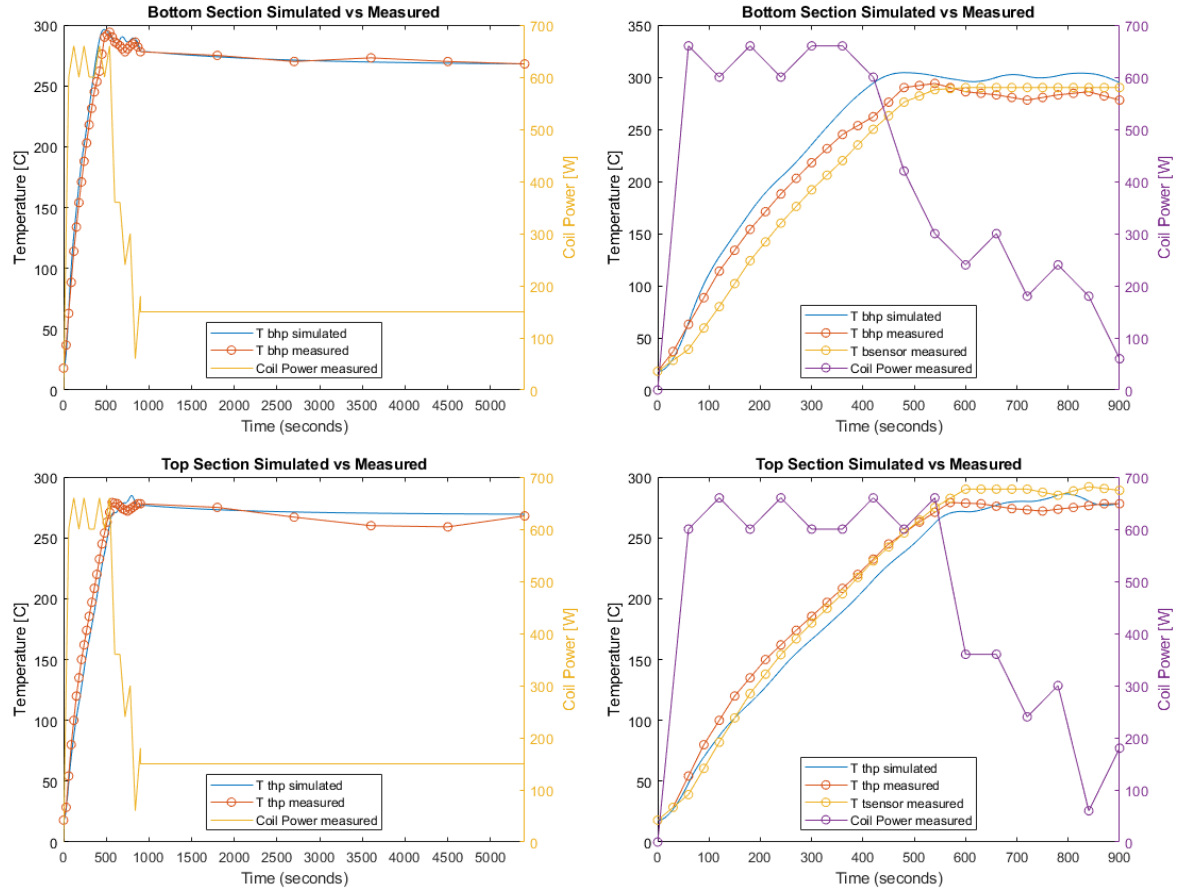

Figure 12 Validation results; Top-Left: Bottom section full; Top-Right: Bottom section heat-up; Bottom-Left: Top section full; Bottom-Right: Top section heat-up

4.1.2. Model Linearization

Figure 13 shows the results of using the tfest function on the simulated input-output data. From these results it becomes clear that this is a 2nd order process because both the transient response and the steady state response are a good visual match. The 4th order match looks perfect, but is actually overfitted and should not be considered.

This process resulted in the transfer functions for the top section and bottom section (13) (14). The step response from 0 to 150W power input showing the response of the linearized against the non-linear system can be seen in Figure 14. While the transient response differs a little, the steady state response which is most important is the same.

$$(15)\ H_{top}(s) = \frac{0.0005174s + 2.864 * 10^{-5}}{s^2 + 0.04162s + 1.625 * e^{-5}}$$

$$(16)\ H_{bottom}(s) = \frac{0.0037s + 2.0203 * 10^{-5}}{s^2 + 0.0213s + 1.1354 * 10^{-5}}$$

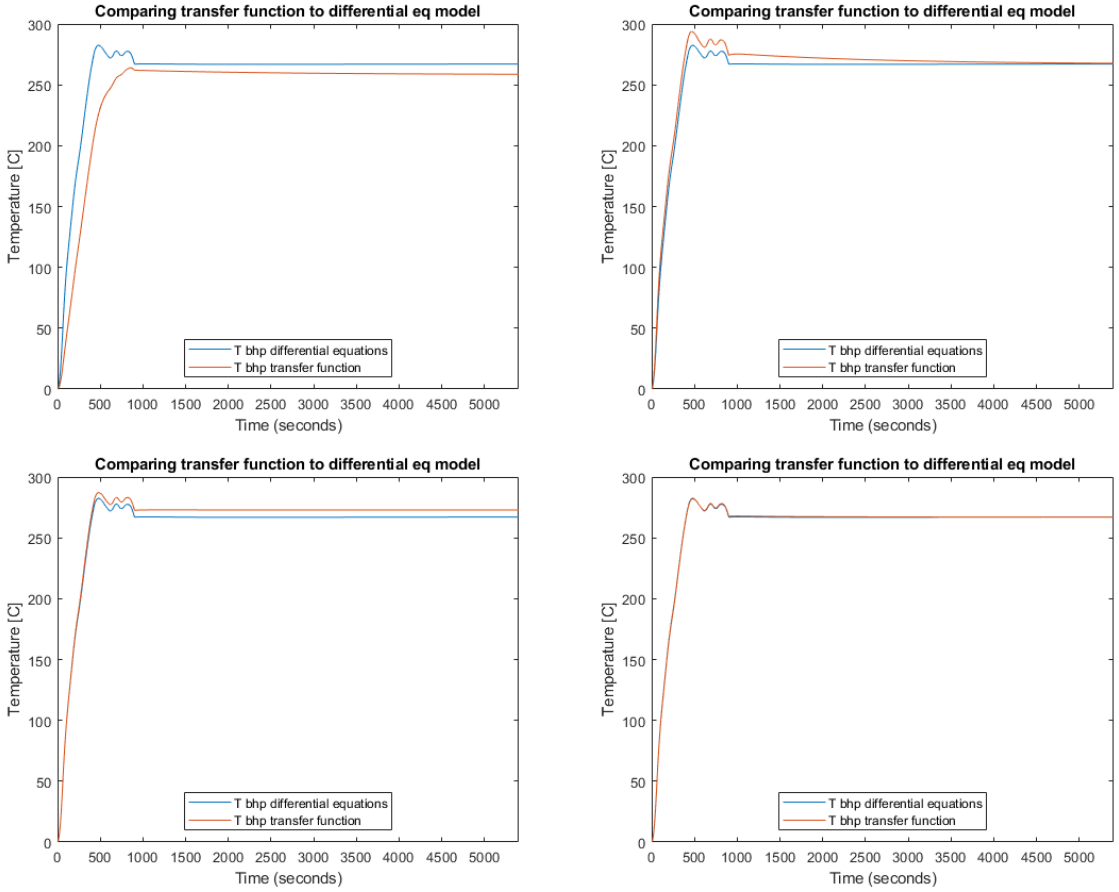

Figure 13 Transfer function fitting results for 1 pole, 2 poles, 3 poles, 4 poles from top-left to bottom-right

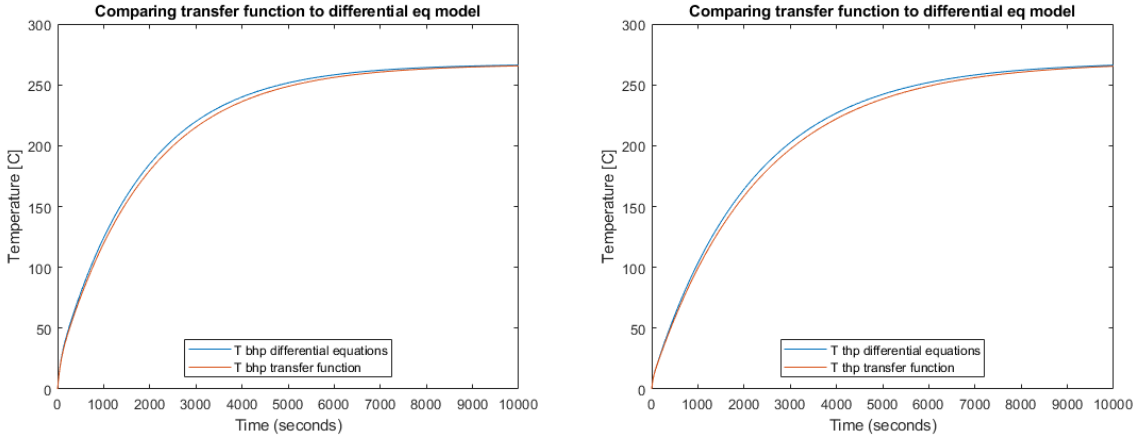

Figure 14 Step response comparison between non-linear and linearized models

4.2 Black box model

For the black box modelling both a 2nd order model was fitted to compare the results with the white box model. A second order assumption seems logical because the mass of the heating element and the mass of the cooking plate heating up can be seen as two first order systems in cascade. Figure 15

shows the resulting black box model and Figure 16 shows a comparison of the step response between the black box model and the white box model.

The best outcome, 91.67% fit, was the following 2nd order system.

$$\frac{3.073e^{-3}s + 1.924e^{-5}}{s^2 + 2.041e^{-2}s + 1.074e^{-5}}$$

Figure 15 2nd order transfer function

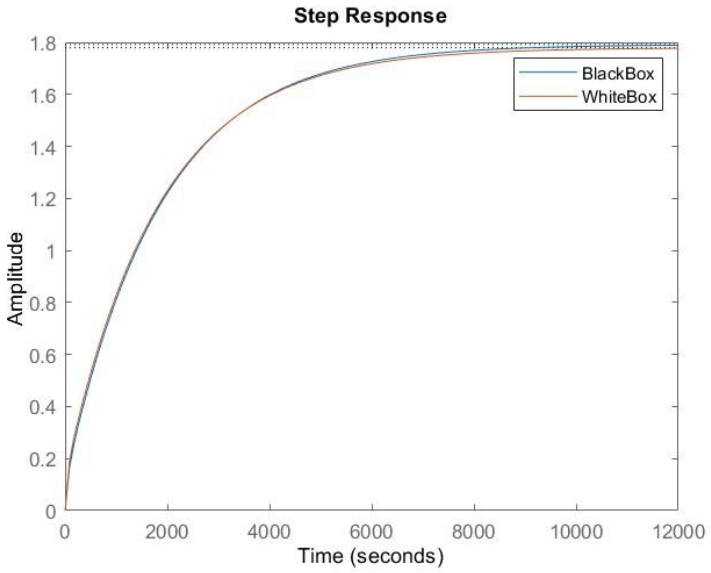

Figure 16 Step response comparison between black box model and white box model

The below figure shows a screenshot of the process. In the *'estimate transfer function'* window the number of poles and zeros are filled in.

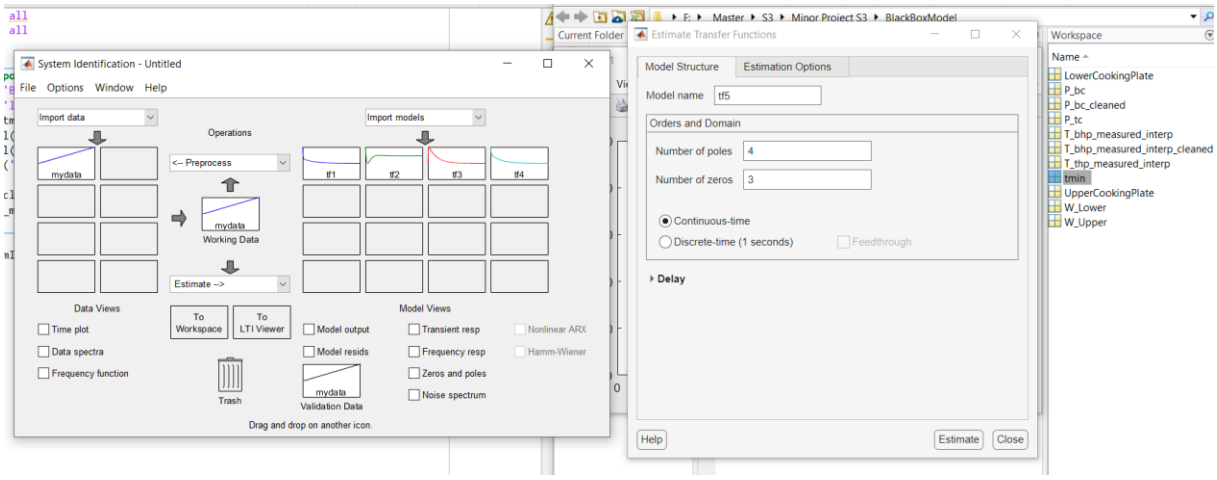

Figure 17 Systems Identification Toolbox

4.3 Controller design

To design the controller a clear understanding of the system and the way in which it behaves is needed. A black box and white box model of the system were created for this purpose. Based on this

information the team derived two transfer functions which represent the behavior of the heating systems which need to be controlled.

The transfer functions are as follows:

- 4th order transfer function: $\frac{0.0030s^3+0.000048978s^2+2.5849*10^{-7}s+4.3592*10^{-10}}{s^4+0.0288s^3+0.00023163s^2+5.8211*10^{-7}s+2.4497*10^{-10}}$
- 2nd order transfer function: $\frac{0.0037s+2.0203*10^{-5}}{s^2+0.0213s+1.1354*10^{-5}}$

A control system was designed for both transfer functions, however based on the nature and behavior of the system when compared to that of the machine, it later became clear that the 4th order transfer function was overfitted and that the 2nd order function was sufficient. Thus, the 4th order system is displayed as a formality. All work with respect to the design of the controller was done based using the 2nd order system.

A root locus plot of the system for the 2nd order system was created to analyze the stability of the system, based on the location of the poles and zeros on the s-plane. The root locus of this system is show below in Figure 18.

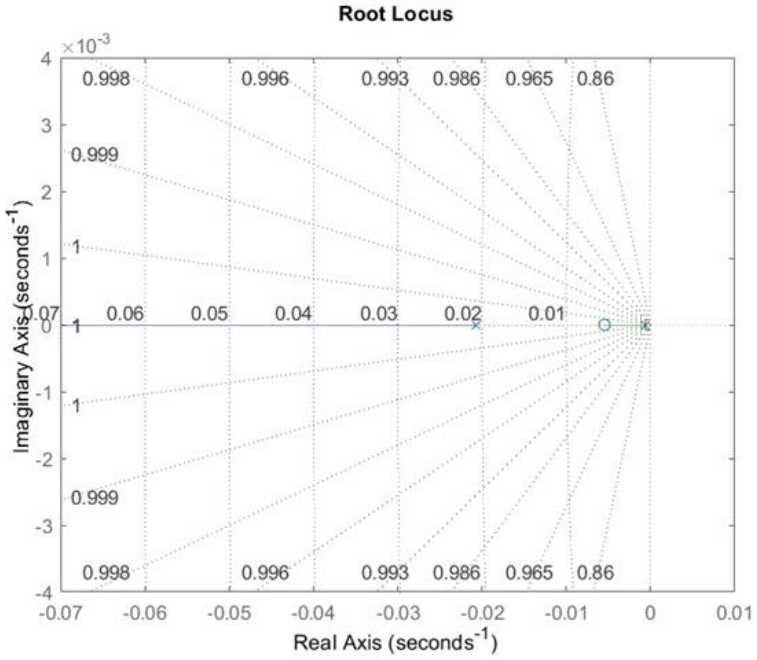

Figure 18 Root locus of the second order transfer function

As can be seen, the poles and zeros of the system are in the left-half side of the s-plane which means that the system is stable and its behavior will decay to a steady state value.

Sensor dynamics and behavior

The behavior the sensor was not taken into account as the sensors response time is assumed to be very quick. This information was not taken from the data sheet, as the supplier does not give specific numbers as it depends on the application. However, it was determined from measurements conducted by the bachelor student working on optimizing the design of the machine that the time constant of the sensor is significantly lower than that of the process [8]. Therefore, sensor dynamics were ignored to simplify the design of the controller.

Type of controller
Based on the behavior of the system the approach for controller design was optimized. As the goals for control during the warm-up phase and the cooking phase of the machine are different. During the warm up phase the control goals are as follows:

- Quick rise time (as quick as possible)
- Low or no overshoot (to prevent damage to the components)
- Quick settling time (so that production can be started as soon as possible)
- Low steady state error

However, during operation, when the machine is making rice waffles, a robust controller is needed with the following control goals:

- Good disturbance rejection
- Quick reactions

Thus to ensure that the performance of the machine is maintained, the team needed to make a trade-off between the two and design a controller that perform sufficiently well in both phases as opposed to performing well in one phase. In the future a two-phase controller could be considered.

Tuning the controller:
Using the 2nd order transfer function, a PI and PID controller were designed and implemented to observe the effect on the system. Disturbances were added to the model to observe the general behavior of the controlled system based on the goals for control. Using the built-in tuner within Simulink the controller parameters were determined based on the response of the system. Finding the correct balance is tricky because a fast rise time could affect overshoot and increasing the robustness affects the transient behavior of the system.

After a few simulations, the preliminary results seemed acceptable and it was decided to us a PI controller because of the following reasons:

- Quick response
- Lower overshoot
- Robust

Furthermore, as we could not account for potential noise in the sensor signal. The team decided a PI controller would be best as there was insufficient time to investigate the effect of the sensor noise on a D action.

Coefficients	PI controller	PID controller 1	PID controller 2
Kp	60	3.7053	16.4395
Ki	0.6	0.0093	0.5015
Kd	-	-232.7504	-2.2304

Table 7 Coefficients for controllers

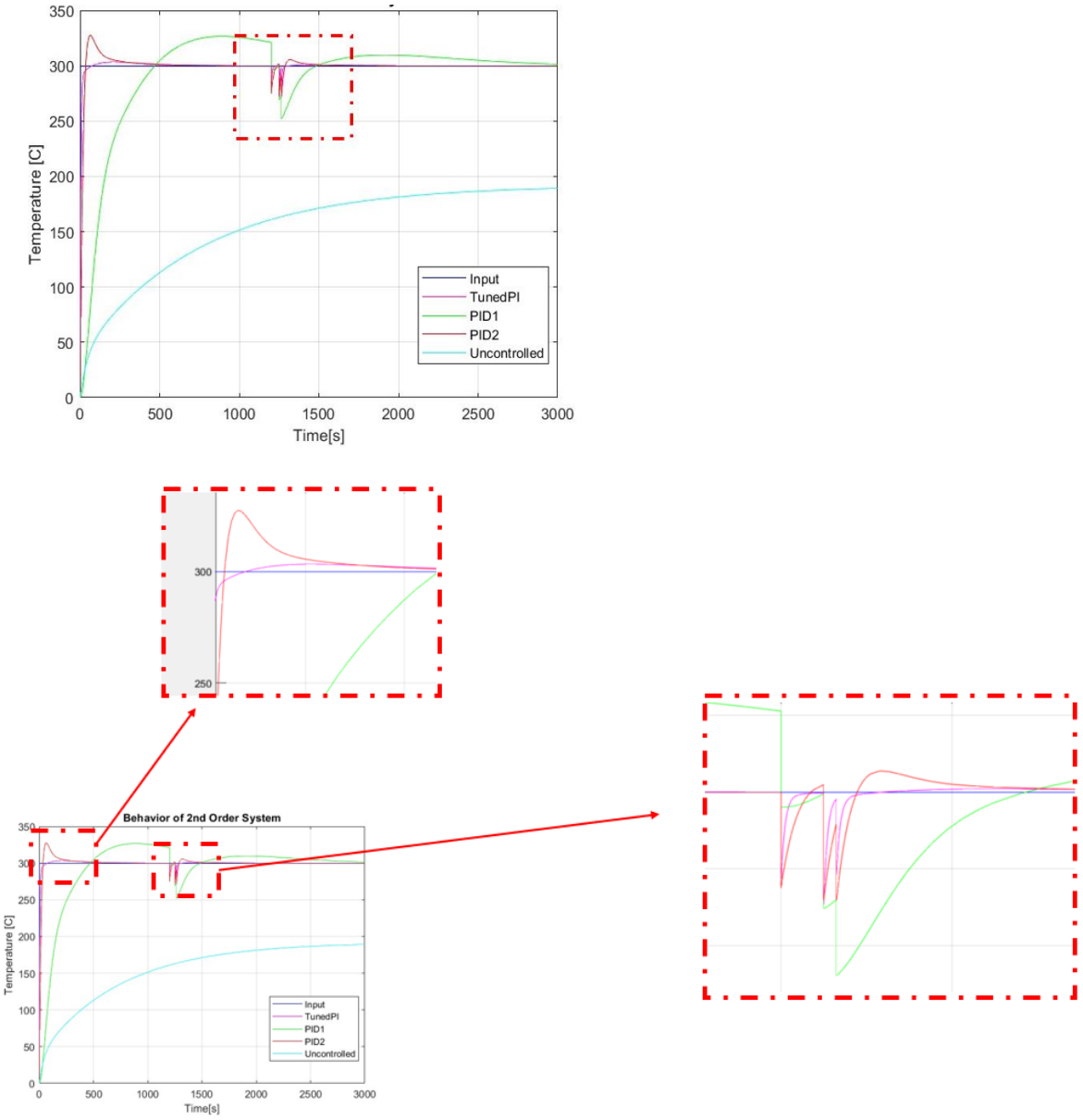

Figure 19 Simulation Results

Figure 19 shows the simulation results. The green line represents the uncontrolled transfer function of the system, the red line represents PID controlled system (with disturbances), the light blue line represents a PI controlled system (with disturbances), the pink line is the second PID tuned controller with different coefficients and the dark blue line is the step input. The red box on the graph shows the area where the disturbances were added

As can be seen from the graph the tuned PI controller gives the best results, due to its quick response time and robustness. It is expected that there will be a difference when testing on the machine as the simulations do not always match reality. However, the values obtained by simulation will provide a starting point for conducting tests on the machine.

4.4 Controller implementation

This paragraph describes the controller implementation as it was built up and tested at the Slagman workshop on the 8th and 9th of June. In short an Olimexino STM32F3 microcontroller [9] is used to run the temperature and pneumatics controls. The existing controls cabinet was decoupled from the

machine and coupled to the test setup described below. For instructions on how to flash the program to the Olimexino or how to start and stop the test setup please see Appendix C.

4.4.1 Hardware implementation

For the implementation of the hardware a list of hardware components was compiled. This list was made based on the characteristics of the components of the test machine and the Olimexino. A detailed list of components used can be found in Appendix E.
The electrical and pneumatic components already in the system between which interfaces are needed are the following:

- 2x Thermocouple type J Tempcontrol TE-8316/S
- 2x Heating element GC Heat
- 6x Electromagnetic pneumatic valve VUVG-B18-B52-ZT-F-1T1L
- 6x Pneumatic cylinder (different sizes)
- 1x Olimexino STM32F3

For the electromagnetic valves a relay is needed for each valve which can switch 24VDC with a 3.3VDC digital output of the Olimexino. For the heating elements solid state relays are needed which can switch 230VAC 5A with 3.3VDC of an Olimexino digital output. Finally to read the thermocouple a 4-20mA transmitter is required in combination with a 4-20mA to 3.3V converter for reading out the sensor on an analog input of the Olimexino. A schematic of the hardware setup is given in Figure 20, and the physical setup in Figure 21. The pin layout for the Olimexino is given in Table 8.

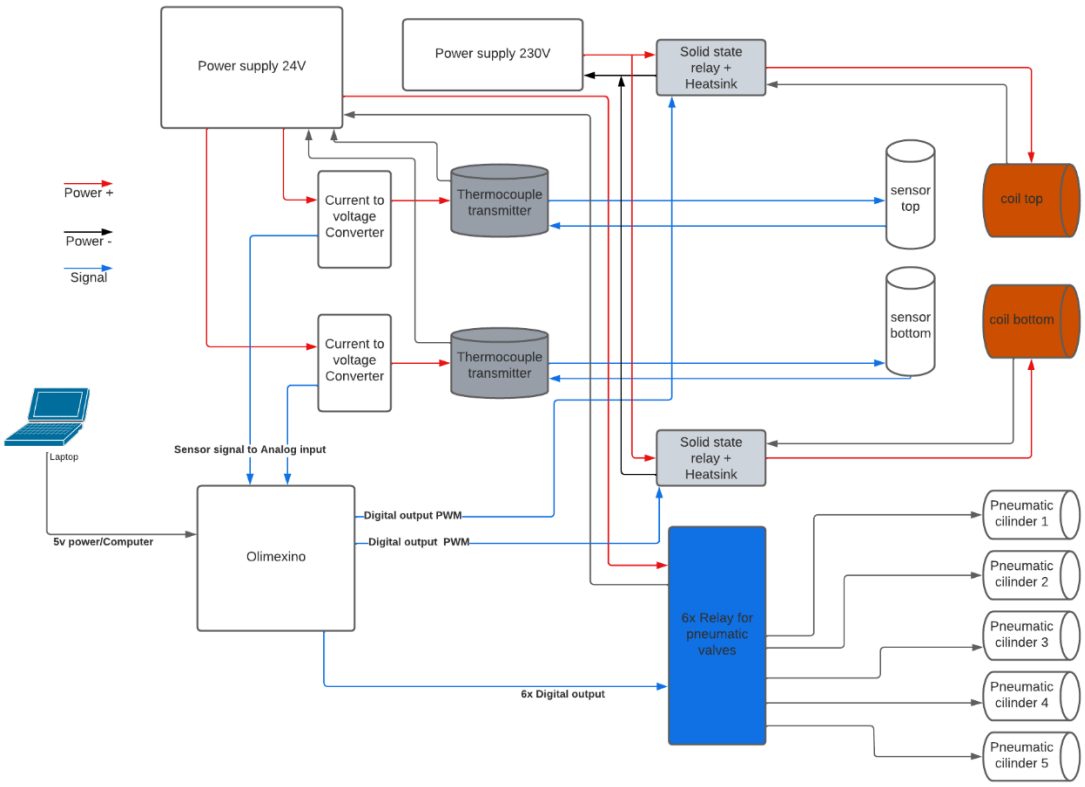

Figure 20 Hardware setup schematic

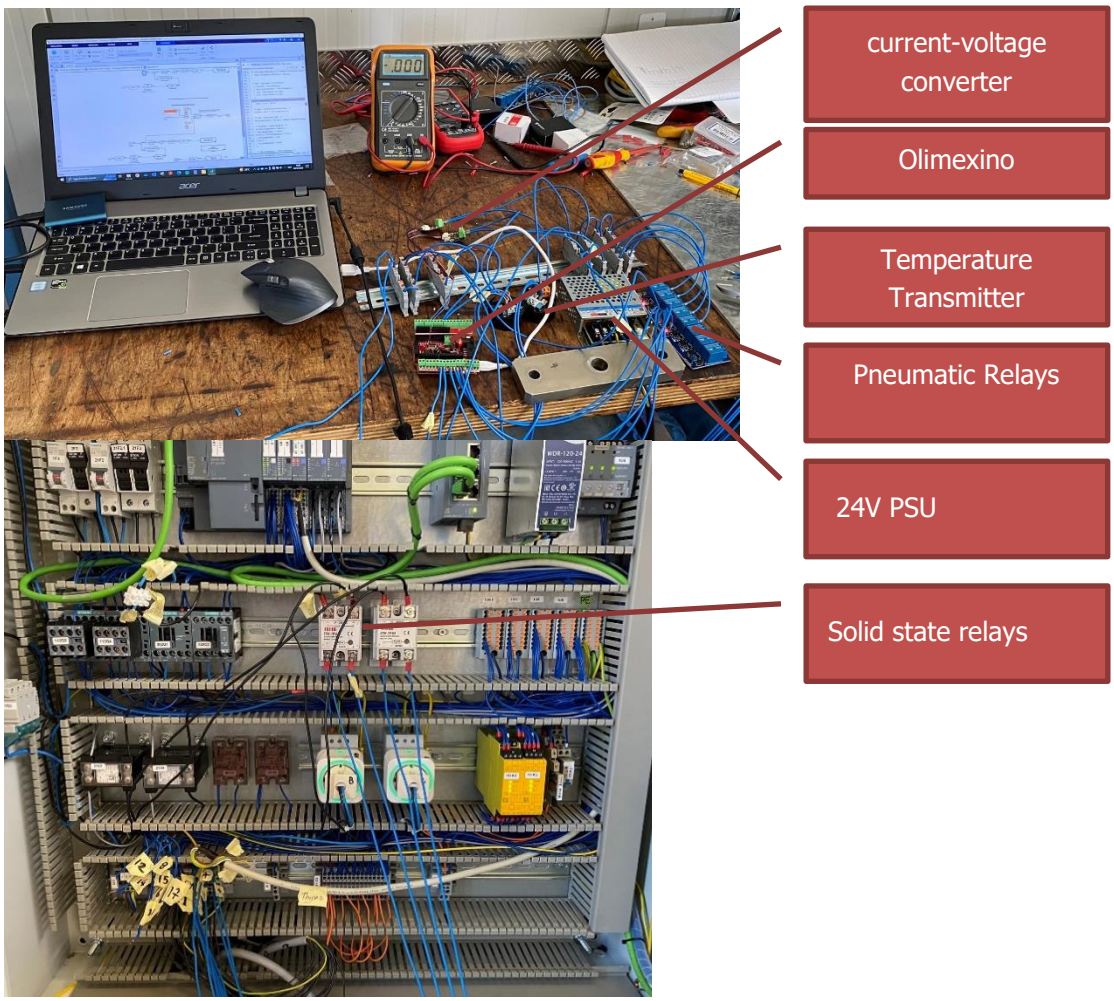

Figure 21 Hardware setup

Olimexino Pin	**Function**
D10	Relay K1 – Claw forward
D11	Relay K2 – Claw open
D9	Relay K3 – Ring down
D12	Relay K4 – Cylinder up
D13	Relay K5 – Cylinder down
D7	PWM output solid state relay top
D6	PWM output solid state relay bottom
A0	Sensor input bottom
A1	Sensor input top

Table 8 Olimexino pin layout

4.4.2 Software implementation

The software is implemented as a Simulink model which is flashed to the microcontroller. The files can be found in Appendix D. The pneumatics control is given in Figure 22. Each relay labelled K1 through K5 is controlled by a repeating pattern which changes every second. The patterns used for testing are given in Table 9. A one in the pattern engages the valve while a zero releases it. The patterns are not optimised and made primarily to follow the correct sequence for demonstration purposes.

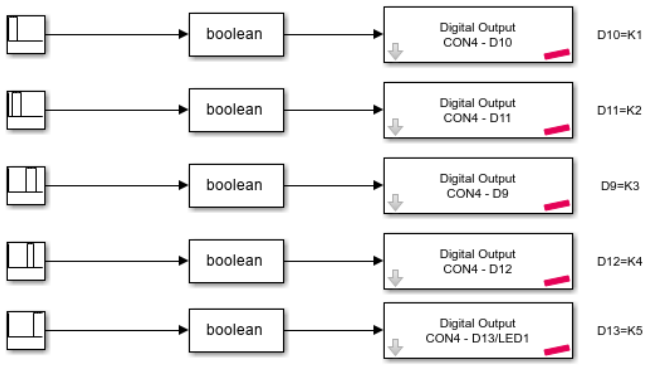

Figure 22 Pneumatics control program

Relay/Valve	**Pattern**
K1/Claw forward	1 1 1 1 0 0 0 0 0 0 0 0 0 0 0 0
K2/Claw open	0 0 1 1 1 1 0 0 0 0 0 0 0 0 0 0
K3/Ring down	0 0 0 0 0 0 0 0 1 1 1 1 1 0 0 0
K4/Cilinder up	0 0 0 0 0 0 0 0 0 1 1 1 0 0 0 0
K5/Cylinder down	0 0 0 0 0 0 0 0 0 0 0 0 1 1 1 1

Table 9 Pneumatic valve patterns

Figure 23 shows the control program for the temperature control which is a feedback loop. There are two of these in the program which are the same for both the top and the bottom section, with the only difference being the corresponding I/O pins. A setpoint can be given, and a PI controller acts on the error temperature between the setpoint and the measurement. The controller outputs the power to be given to the coils, this is converted to a duty cycle by (16). The sensor is measured on a 12 bit ADC which is first converted to a voltage by (17), then the voltage is converted to a temperature by (18) [10].

$$(16)\ \%_{duty} = u\frac{660}{1023}, where\ u\ is\ the\ controller\ output$$

$$(17)\ y = u\frac{3.3}{4095}$$

$$(18)\ y = \frac{u-0.48}{2.4-0.48}300$$

The PI controller has a clamping anti windup enabled because the process takes a long time to reach the setpoint when warming up, and the actuator cannot output more than 660W at a 100% duty cycle. It is a discrete system with the Olimexino acting also as the ADC and DAC. The integration method is backward Euler rather than the default forward Euler because the system is real-time.

Finally a low-pass filter with a cutoff frequency at 2Hz can be seen. The cutoff frequency was determined experimentally by getting to a steady state situation where the setpoint is equal to the measurement, and observing when the error is positive or negative through the LED on the microcontroller. Without a filter there is a lot of flickering which causes unnecessary heating and a large steady state error. This filter filters out the noise and leaves only the slow changing sensor signal for the feedback loop to act on.

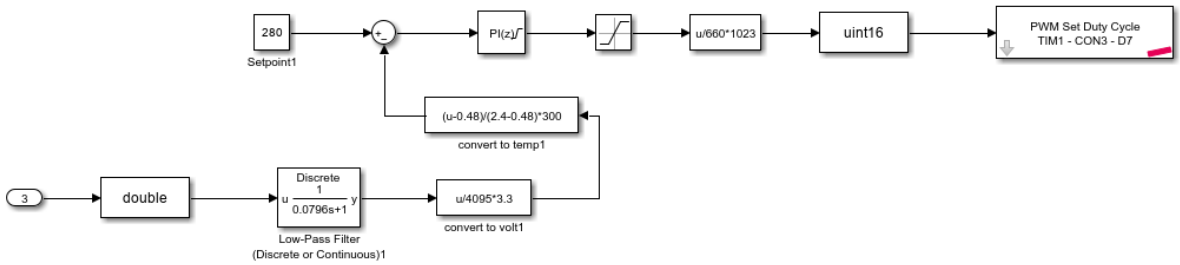

Figure 23 Temperature control program

4.4.3 Sensor measurement validation

The controller will take measurements from the machine's type J thermocouple temperature sensors. After connecting the thermocouple the voltage on the Olimexino analog input is measured with a multimeter and converted to a temperature [10]. Throughout the testing period at various points this temperature was compared to a temperature measured by a thermometer held to the side of the cooking plates. The temperature on the side of the cooking plate lags behind the temperature measured by the sensor which is located in the center. However, after some time they are roughly the same. Taking measurements in this way it was determined that the temperature measurement is accurate within 2 degrees.

(19) $T = \frac{V_{measured} - 0.48}{2.4 - 0.48} * 300$

4.4.4 Actuator output validation

The controller will control the power delivered to the heating coil by setting the duty cycle of a PWM signal. The PWM signal switches a solid state relay which controls the current flowing to the heating coil. To validate the actuator output, for various duty cycles the power output was measured using a Voltcraft SEM6000 energy meter. The results are summarized in Table 10. The maximum switching frequency for the used solid state relays is 100Hz. With a frequency of 50Hz lower duty cycles do not work properly. A frequency of 10Hz was selected which allows duty cycles as low as 5%, although for lower duty cycles the power output remains the same.

Duty Cycle [%]	Frequency [Hz]	Power [W]
100	50	660
50	50	330
10	50	0
10	10	66
5	10	66
1	10	0

Table 10 Actuator test results

4.4.5 Controller tuning

To tune the controller values first Ziegler-Nichols was considered, but the method of Chien, Hrones and Reswick was used in the end. Both methods are discussed in paragraph 2.4. Ziegler-Nichols requires the system to be brought to a state of constant oscillation, but practically for the system at hand this proved impossible to create and measure, and it was also a time-consuming method. The method of Chien, Hrones and Reswick is based on a step-response measurement of the open-loop system going from one operating point to another, which was possible to realize.

First the open-loop system was given a constant duty cycle of 10%, and it reached a steady state temperature of 152ºC with an ambient temperature of 30ºC. Then the duty cycle was given a step to 20% and the resulting response which was measured for about half an hour is shown in Figure 24. Unfortunately the full response could not be measured due to a lack of time.

Since the full step response could not be measured the controller values were determined by a slope-based method instead [7]. The dead time measures 60 seconds when looking at the sensor voltage with 2 significant digits. The slope is measured as 2 degrees temperature change per 30 seconds. The calculated P & I values are given below (19) (20).

(20) $P = 1.2V_{max}\, T_u \frac{y_H}{\Delta y} = 48$

(21) $I = 3.3T_u = 198$

where V_{max} *is the slope,* T_u *is the deadtime,* y_H *is the maximum adjustment range* (100%), Δy *is the step change* (10%)

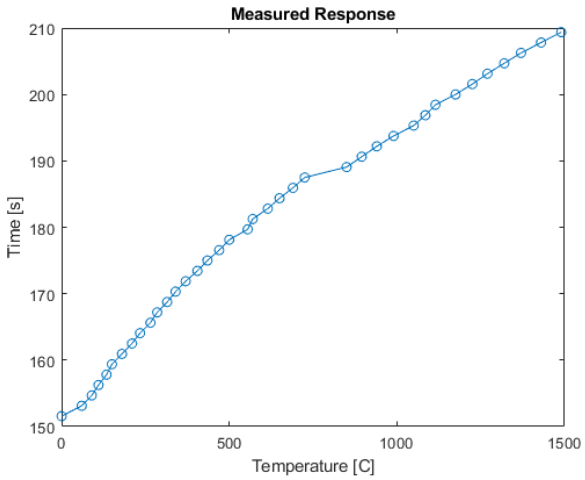

Figure 24 Step Response open-loop from 10% to 20% duty cycle

4.4.6 Controller validation

Initially the theoretically designed controller settings were tried. While they managed to heat up the element the resulting response was slow and there was a significant overshoot / steady state error of around 15ºC which could not be reduced quick enough by the I action. Afterwards the controller settings were experimentally tuned and with these settings the steady state error was gone and the controller was able to stay around the setpoint (within a band of around 3 degrees) in a steady state situation with no production.

Due to a lack of time there are no detailed measurements collected for the complete controller, but instead a test run was performed where the microcontroller completely took over both the pneumatic and thermal controls from the control cabinet. The system was brought up to an operating temperature of 280ºC and then loaded with rice. Rice waffles were successfully produced with a quality and yield at least as good as the original control cabinet. The process ran for around 5 minutes until the rice depleted, and the resulting waffles can be seen in Figure 25.

During the process the temperature was monitored by measuring the thermocouple output with a multimeter and it fluctuated between 279ºC and 289ºC. This indicates that the current tuning is likely too aggressive and overshoots whenever it drops below the setpoint. This is consistent with the high calculated I value as compared to the theoretically designed controller values.

Figure 25 Resulting wafers

5. CONCLUSIONS

In this study a temperature and pneumatics control system for the rice popping process was successfully designed and implemented, considering its thermal dynamics and mechanical characteristics. The thermal controller uses a feedback loop with PI controller while the pneumatics controller is open-loop. To design and simulate the controller a thermal model of the system was developed both using white box and black box modelling methods. The controller was implemented, tuned, and validated on the test machine setup in the workshop at Slagman. With this prototype setup rice wafers were successfully made with the temperature fluctuating between 279ºC and 289ºC which is significantly less than with the original controller.

The developed control system, comprising the thermal model, open-loop pneumatic system, and tuned PI controller, provided effective temperature regulation and control. The Simulink implementation facilitates a thorough analysis of the system's behavior and allows for optimization of the control parameters. This research lays the foundation for further advancements in rice popping process control.

To optimize the temperature control of the Slagman machine, which is essential for maximizing the production yield of rice waffles and reducing energy consumption, the characteristics and requirements of the system were addressed by the four research questions. The findings are summarized in the following points.

1. The popping process of rice waffles in the Slagman machine involves crucial parameters such as the initial moisture content of the rice, cooking time, pressure, and temperature profile. These parameters directly impact the texture, flavor, and quality of the final product, hence the need to understand the optimal ranges for these parameters and analyze the effects of variations in these parameters to help determine the optimal conditions for maximum production yield and energy efficiency.
2. To regulate the temperature and achieve precise control while the machine is in operation, we employed a PI controller. The controller's parameters were tuned using the root locus method, which allowed us to analyze the system's stability and adjust the controller's gains accordingly. For the implementation a slope-based tuning method was employed.
3. Ensuring the robustness of the temperature control system was crucial to handle uncertainties and disturbances that arise during the popping process. Robustness analysis was conducted to evaluate the controller's performance under various scenarios. This analysis helped in validating the effectiveness of the PI controller to effectively handle variations and uncertainties, ensuring reliable and accurate temperature control.
4. Improving temperature control in the Slagman machine has a significant impact on the process cycle of rice waffle production. Precise temperature regulation leads to consistent cooking and texture of the rice waffles, reducing batch-to-batch variations and ensuring high-quality output. Additionally, optimizing the temperature control will minimize energy consumption by avoiding excessive heating and temperature overshoot. This optimization will ultimately result in cost savings and increased energy efficiency, contributing to the overall sustainability of the process.

6. RECOMMENDATIONS

To continue the progress and further improve the design and performance of the controller these are the recommendations which Slagman could implement when moving forward in the next iteration of the controller design.

- Create a standalone controls cabinet for use with the Olimexino microcontroller. This control cabinet should work autonomously and have its own test plug so that it can be used with any test poffer.
- Improve the tuning of the controller values:
    - The top and bottom section should be tuned independently.
    - An accurate step response should be measured to apply the Chien-Hrones-Reswick method.
    - Investigate the use of a D action.
- Improve the Olimexino program:
    - Log process values to an SD card or display them to aid taking measurements.
    - Improve the pneumatics control program to allow for easy timing adjustments.
- Investigate using feedback control for the main pneumatic cylinder.
- Investigate using a two-phase controller with a separate tuning for the warmup and cooking phase, since they have different requirements. This would only have a small effect on efficiency as it only impacts the startup phase.
- Investigate using a feedforward controller to preempt the rice cooking. Since it is a known disturbance this could improve disturbance rejection.
- Investigate the sensor dynamics / delays so that the control can be based on the cooking plate surface temperature rather than the sensor temperature.
- Test the controller with machines with varying run-hours, dirtiness, disturbances, and components.

7. REFERENCES

[1] E. Tazelaar, C. Stroomer and B. Veenhuizen, *An Introduction to Modeling Dynamics,* Arnhem: HAN, 2016.

[2] M. Boerlage, M. Steinbuch, P. Lambrechts and M. van de Wal, "Model-based feedforward for motion systems," in *2003 IEEE International Conference on Control Applications (CCA)*, Istanbul, Turkey, 2003.

[3] G. Na, H. JingTao and W. He, "Intelligent operation control system for rice transplanter based on GPS navigation.," *Transactions of the Chinese Society for Agricultural Machinery,* vol. 44, no. 1, pp. 200-204, 2013.

[4] D. Ruicheng, G. Bingcai, L. Ningning, W. Chenchen, Y. Zidong and M. Mingjian, "Design and experiment on intelligent fuzzy monitoring system for corn planters," *International Journal of Agricultural and Biological Engineering,* vol. 6, no. 3, 2013.

[5] LibreTexts, "PID Tuning via Classical Methods," [Online]. Available: https://eng.libretexts.org/Bookshelves/Industrial_and_Systems_Engineering/Chemical_Process_Dynamics_and_Controls_(Woolf)/09%3A_Proportional-Integral-Derivative_(PID)_Control/9.03%3A_PID_Tuning_via_Classical_Methods. [Accessed 14 June 2023].

[6] R. Sen, C. Pati, S. Dutta and R. Sen, "Comparison Between Three Tuning Methods of PID Control for High," *Journal of Metrology Society of India,* vol. 30, no. 1, pp. 65-70, 2015.

[7] Jumo, "PID Regelaar - De meest gestelde vragen over PID regelaars," [Online]. Available: https://www.jumo.nl/web/services/faq/controller/pid-controller#hoewordtdepidregelaargeoptimaliseerd. [Accessed 14 June 2023].

[8] J. Lankhorst, "Thermal System Description," Slagman Techniek B.V., Doetinchem, 2023.

[9] Olimex, "OLIMEXINO-STM32F3," [Online]. Available: https://www.olimex.com/Products/Duino/STM32/OLIMEXINO-STM32F3/open-source-hardware. [Accessed 14 June 2023].

[10] DFRobot, "Gravity Analog Current to Voltage," [Online]. Available: https://wiki.dfrobot.com/Gravity__Analog_Current_to_Voltage_Converter_for_4~20mA_Application__SKU_SEN0262#More_Documents. [Accessed 14 June 2023].

[11] OpenMDB, "HANcoder," [Online]. Available: https://openmbd.com/hansuite/. [Accessed 14 June 2023].

[12] LibreTexts, "P, I, D, PI, PD, and PID Control," [Online]. Available: https://eng.libretexts.org/Bookshelves/Industrial_and_Systems_Engineering/Chemical_Process_Dynamics_and_Controls_(Woolf)/09%3A_Proportional-Integral-Derivative_(PID)_Control/9.02%3A_P%2C_I%2C_D%2C_PI%2C_PD%2C_and_PID_control. [Accessed 14 June 2023].

APPENDIX A WHITE BOX MODEL PARAMETERS

The table below lists the symbols, descriptions, and sources of the white box model parameters. The symbol notation as it is used in the Matlab files is used.

Symbol	Description	Value	Unit	Source
diameter_cilinder	Diameter of the modelled cilinder	0.092	m	3d model
area_cilinder	Area of the top/bottom of the modelled cilinder	0.0066	m^2	calculated
density_m	Material density metal Bohler M340; used for metal and heating plate layers.	7700	kg/m^3	[8]
c_tm	Specific heat capacity top metal layer	460	J/(kgC)	[8]
k_tm	Thermal conductivity top metal layer	22	W/(mC)	[8]
d_tm	Thickness top metal layer	0.035	m	3d model
m_tm	Mass top metal layer	1.7915	kg	calculated
A_tm	Area of the top/bottom of the top metal layer	0.0066	m^2	calculated
A_tm_air	Area of the side of the top metal layer	0.0101	m^2	calculated
c_bm	Specific heat capacity bottom metal layer	460	J/(kgC)	[8]
k_bm	Thermal conductivity bottom metal layer	22	W/(mC)	[8]
d_bm	Thickness bottom metal layer	0.035	m	3d model
m_bm	Mass bottom metal layer	1.7915	kg	calculated
A_bm	Area of the top/bottom of the bottom metal layer	0.0066	m^2	calculated
A_bm_air	Area of the side of the bottom metal layer	0.0101	m^2	calculated
density_c	Material density of the coil; Metal CrNi which is assumed to have similar properties as Bohler M340	7700	kg/m^3	assumed
length_c	Length of the coil	0.9	m	datasheet
w_c	Width of the coil	0.0042	m	datasheet
h_c	Height of the coil	0.0022	m	datasheet
c_tc	Specific heat capacity top coil layer	460	J/(kgC)	assumed
m_tc	Mass top coil layer	0.064	kg	calculated
c_bc	Specific heat capacity bottom coil layer	460	J/(kgC)	assumed
m_bc	Mass bottom coil layer	0.064	kg	calculated
c_thp	Specific heat capacity top heating plate layer	460	J/(kgC)	[8]
k_thp	Thermal conductivity top heating plate layer	22	W/(mC)	[8]
d_thp	Thickness top heating plate layer	0.01	m	3d model
m_thp	Mass top heating plate layer	0.5119	kg	calculated
A_thp	Area of the top/bottom of the top heating plate layer	0.0066	m^2	3d model

A_thp_air	Area of the side of the top heating plate layer	0.0029	m^2	calculated
c_bhp	Specific heat capacity bottom heating plate layer	460	J/(kgC)	[8]
k_bhp	Thermal conductivity bottom heating plate layer	22	W/(mC)	[8]
d_bhp	Thickness bottom heating plate layer	0.01	m	3d model
m_bhp	Mass bottom heating plate layer	0.5119	kg	calculated
A_bhp	Area of the top/bottom of the bottom heating plate layer	0.0066	m^2	3d model
A_bhp_air	Area of the side of the bottom heating plate layer	0.0029	m^2	calculated
density_r	Material density of the ring, Bohler W302	7800	kg/m^3	[8]
c_r	Specific heat capacity ring	470	J/(kgC)	[8]
k_r	Thermal conductivity ring	22.8	W/(mC)	[8]
d_r	Thickness ring	0.0075	m	3d model
h_r	Height ring	0.0245	m	3d model
m_r	Mass ring	0.448	kg	calculated
A_r_air	Area of the ring exposed to air	0.0196	m^2	calculated
A_r_tm	Area of the ring overlapping with the metal	0.0042	m^2	calculated
h_c	Convective heat transfer coefficient, the top and bottom sections use a different value.	16.5 top 26.5 bottom	$W/(m^2C)$	determined experimentally

APPENDIX B WHITE BOX MODEL VALIDATION DATA

The table below shows the validation data which was provided by [8]. For both the top section and bottom section the input power and heating plate temperature are given.

Time [s]	$P_{tc}[W]$	$T_{thp}[C]$	$P_{bc}[W]$	$T_{bhp}[C]$
0	0	18	0	18
30		28.5		36.95
60	600	54.25	660	63
90		80		88.5
120	660	100	600	114
150		120		134
180	600	135	660	154
210		150		171
240	660	162	600	188
270		175		203
300	600	185.5	660	218
330		197		231.5
360	600	208.5	660	245
390		220		253.5
420	660	232.5	600	262
450		245		276
480	600	254	420	290
510		263		292
540	660	271	300	294
570		279		290
600	360	278.5	240	286
630		278		284.5
660	360	276	300	283
690		274		280.5
720	240	273	180	278
750		272		280.5
780	300	273.5	240	283
810		275		284.5
840	60	276.5	180	286
870		278		282
900	180	278	60	278
1800	150	275	150	275
2700	150	267	150	270
3600	150	260	150	273
4500	150	259	150	270
5400	150	268	150	268

APPENDIX C PROCEDURES FOR USING THE TEST SETUP

This appendix lists the procedures for programming the Olimexino as well as for starting- and stopping the test setup as it is built up in the Slagman workshop.

Programming Procedure

For loading the Matlab Simulink program onto the Olimexino HANcoder v2.1 is used. For information on setting up the environment for using HANcoder the website can be consulted [11]. Once the environment is setup, then building the code for the Simulink model will automatically update the Olimexino which is connected to your machine. For this to work the Olimexino should be in bootloader mode which is entered by pressing both buttons on the board.

Starting Procedure

1. Power up the Olimexino using a USB cable

2. Power up the test cabinet. IMPORTANT TO NOTE: While the test cabinet is powered, until the 24V supply is connected the heating coils will heat at full power unregulated. This happens because there is no sensor signal until the 24V supply is turned on. While the 24V supply is turned on the controller will stop the heating process when the setpoint is reached.

3. Power up the external 24V power supply. IMPORTANT TO NOTE: As soon as the 24V supply is turned on the pneumatics system will immediately start following the sequence, no matter where in the sequence the relays are.

Stopping Procedures

1. Power off the external 24V power supply. IMPORTANT TO NOTE: While the test cabinet is still powered on, the heating coils will heat at full power unregulated.

2. Power off the test cabinet.

3. Power off the Olimexino. IMPORTANT TO NOTE: As soon as the Olimexino is powered down, all pneumatic valves will be switched on if the 24V power supply is still connected.

APPENDIX D MATLAB FILES

The following Matlab files were included together with this report in a zip file.

White Box Modelling Simulink

This folder contains all files used for the white box modelling. model.xls is the Simulink model and main.m is the script used to run it. This script should be ran section-by-section.

Black Box Modelling Simulink

This folder contains all the files used for the black box modelling. BBModel.m is the main script used to fit the model to the data.

Controller Design Simulink

This folder contains all the files used for the controller design. It consists of various scripts and Simulink models.

Realization Simulink

This folder contains the files used for the realization. HANcoder_olimexino_F3.slx is the Simulink model to be loaded to the Olimexino.

APPENDIX E COMPONENT LIST

The table below lists the components used for the prototype setup.

Description	URL	Amount
Solid state relay for driving coil	https://www.vanallesenmeer.nl/Solid-state-relais-3-32V-/-10A-/-24-380VAC-SSR-10-DA	3
Heatsink for solid state relay	https://www.vanallesenmeer.nl/Solid-state-relais-Heatsink	2
Relay for driving the valves	https://www.vanallesenmeer.nl/5VDC-Relais-board-8-kanaals	2
4-20 mA to 5V converter for sensor	https://opencircuit.nl/product/gravity-analog-current-naar-voltage?srsltid=AR57-fC5LN2VGuFlRIsXX9qwv3tHJmoFiPr3Y8MQMpPsGzW_gRjNWPLQU9o	1
24VDC power supply for valves	https://www.conrad.nl/nl/p/dehner-elektronik-lm50-20b24-schakelnetvoeding-2-2-a-50-w-24-v-gestabiliseerd-1-stuk-s-2361728.html	1
230V cable and plug for coils	https://www.conrad.nl/nl/p/basetech-xr-1638085-stroom-aansluitkabel-zwart-5-00-m-2182184.html	1
Terminals for connecting power supply to relays	https://www.conrad.nl/nl/p/phoenix-contact-pt-2-5-quattro-3209578-doorgangsklem-aantal-polen-4-0-14-mm-2-5-mm-grijs-1-stuk-s-733395.html	10
Terminal bridges	https://www.conrad.nl/nl/p/fbs-2-5-steekbrug-fbs-2-5-phoenix-contact-inhoud-1-stuk-s-673821.html	5
DIN rail	https://www.conrad.nl/nl/p/rittal-sz-ts35-7-5-2317000-din-rail-geperforeerd-plaatstaal-387-mm-1-stuk-s-521016.html	1
thermocouple transmitter	https://nl.rs-online.com/web/p/temperature-transmitters/1852341	2
3x fuse coil	https://www.conrad.nl/nl/p/siemens-3nc10060mk-cilinderzekeringmodule-6-a-690-v-1-stuk-s-1702465.html	3
screw shield header	https://www.vanallesenmeer.nl/Files/2/38000/38789/Enoza/38789_Header_nl.jpg	1
Olimexino microcontroller	https://www.olimex.com/Products/Duino/STM32/OLIMEXINO-STM32F3/open-source-hardware	1